

## Predictive modelling of L-H transition in ITER 15 MA Q = 10 plasma

Hyun-Seok Kim<sup>1</sup>, Vassili Parail<sup>2</sup>, Luca Garzotti<sup>2</sup>,  
Florian Koechl<sup>3</sup>, Alberto Loarte<sup>4</sup> and Yong-Su Na<sup>1\*</sup>

<sup>1</sup>*Deapartment of Nuclear Engineering, Seoul National University, Seoul, 151-744, Korea*

<sup>2</sup>*EURATOM/CCFE Fusion Association, Culham Science Centre, Abingdon, Oxon, OX14 3DB, UK*

<sup>3</sup>*Association EURATOM-Ö AW/ATI, Atominstitut, TU Wien, Vienna, Austria*

<sup>4</sup>*ITER Organization, Saint Paul lez Durance Cedex, France*

\*ysna@snu.ac.kr

A fully self-consistent predictive simulation of the typical ITER 15 MA scenario with  $Q = 10$ , which is based on the type-I ELM/H-mode discharge, is performed for the flat top phase of the scenario starting from the end of current ramp-up phase using the GLF23 and the Bohm/gyroBohm transport model implemented in JINTRAC<sup>1</sup>. This work has a purpose to investigate the characteristic time delay ( $\tau_{\text{delay}}$ ) of reaching the burning conditions with  $Q = 10$  through L-H transition after onset of full heating. Therefore, the sensitivity parametric scans are carried out with the variation of pellet fuelling rate ( $\Gamma_{\text{pellet}}$ ,  $dn_e/dt$ ), inward particle pinch (V), and particle diffusivity (D).

**Simulation Set-up.** The condition of L- to H-mode transition is prescribed using by reducing the heat transport within the edge barrier region to the neoclassical level when the heat flux to the separatrix exceeds the multi-machine experimental power threshold scaling<sup>2</sup>. Two kinds of approach for the description of inherently transient phenomena like pellet ablation and type-I ELM are used: continuous and discrete description. The continuous description<sup>3</sup> is needed in case when using the GLF23 model, which often fails during fast transients. The critical normalised pressure gradient  $\alpha_{\text{cr}}$  is assumed to be a constant consistent with the EPED model prediction<sup>4</sup> for simulating the type-I ELMs. In the pellet simulation, the deposition profile and the injected speed are determined by the HPI2 ablation code. They are assumed to be  $\rho_{\text{pellet}} = 0.85-0.87$  and  $V_{\text{pellet}} = 5 \text{ km/s}$ , respectively. The spherical pellet with  $r_{\text{pellet}} = 0.286 \text{ mm}$  is injected with corresponding to the cubic 5 mm side of fuelling pellet in ITER. The wall recycling is set to zero, because the evolution of the plasma density in this simulation is limited to the region inside separatrix and the cold neutrals are not expected to penetrate effectively through the SOL in ITER discharges.

**Simulation Scheme.** Firstly, a steady state physics-based solution is produced for ITER 15 MA H-mode plasma with  $Q = 10$  by applying the GLF23 model, continuous ELM model, and continuous pellet injection model. The physics-based solution of  $Q=10$  ITER plasma can be obtained in the conditions of  $\Delta_{ETB} = 10$  cm,  $\alpha_{cr} = 2.0$ ,  $\Gamma_{pellet} = 3.0 \times 10^{22} \text{ s}^{-1}$ ,  $P_{NBI} = 33$  MW, and  $P_{RF} = 7$  MW. Then, in order to get similar solution with the Bohm/gyroBohm model compared to the GLF23 model case, the transport multipliers in Bohm/gyroBohm model are manipulated. Then, this solution obtained by using Bohm/gyroBohm model is going to be closer to physics-based. It makes the computing time fast and stable in the calculation of ELM and pellet injection. Next, the L-H transition is simulated starting from the L-mode phase at the end of the current ramp-up to the H-mode phase in the steady state including the dithering phenomena by using Bohm/gyroBohm model, discrete ELM model, and discrete pellet injection model. Finally, the sensitivity scans to investigate characteristics of L-H transition are explored by varying  $dn_e/dt$  and the magnitude of particle inward pinch (V) and particle diffusivity (D) but keeping the ratio of V and D the same.

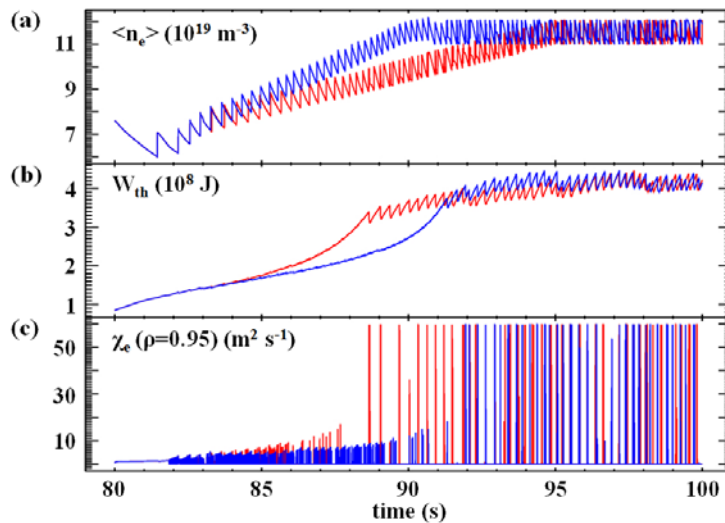


**Figure 1.** The effect of  $dn_e/dt$  on  $\tau_{delay}$  of L-H transition; (a) volume-averaged electron density, (b) plasma stored energy, and (c) electron heat diffusivity in the cases of low  $dn_e/dt$  (red colour) and high  $dn_e/dt$  (blue colour).

**Result and Discussion.** Figure 1 represents the effect of  $dn_e/dt$  on the characteristic time delay ( $\tau_{delay}$ ) in L-H transition with  $P_{NBI} = 33$  MW and  $P_{RF} = 20$  MW. In this simulation, the pellet fuelling is automatically adjusted by feedback control of the volume-averaged electron density. The red one shown in figure 1 is the reference simulation presented in this paper. It shows  $\tau_{delay}$  of about 7 seconds. As shown in Fig. 1 clearly, variation of  $dn_e/dt$  makes difference in L-H transition characteristics. High  $dn_e/dt$  (blue colour in Fig. 1) results in longer  $\tau_{delay}$  and it needs

more time to achieve steady state  $W_{th}$  compared to the low  $dn_e/dt$  case. The explanation to this delay could be that to reheat/maintain high plasma temperature plasma requires more time for the sudden increased plasma density in the higher  $dn_e/dt$  case.  $Q_{DT}$  has shown the similar trend. From this result, characteristic time delay and fusion power increase can be controlled by pellet fuelling speed.

In the purpose of understanding effects of particle diffusivity (D) and particle pinch (V) to the L-H transition, D and V profiles are scanned by multiplying both by some ad hoc factor, but keeping V/D the same as V/D = 0.6 to make similar electron density profile in stationary conditions. Figure 2 shows not only the variation of V and D profiles used for the sensitivity scan but also the effect of (V, D) on  $\tau_{delay}$  in L-H transition. In Fig. 2 (a)-(c), the particle diffusivity multiplier are 0.5, 2.5 and 5.5. The particle pinch profile is also varied by keeping V/D = 0.6. From Fig. 2 (d)-(g), even in the same value of  $dn_e/dt$ , as increasing the magnitude of (V, D) profiles,  $\tau_{delay}$  is increased gradually. It is because the variation of (V, D) makes different pellet fuelling. As shown in Fig. 2 (h), the higher value of (V, D), the more pellets are forced to inject to the plasma by the feedback controller.

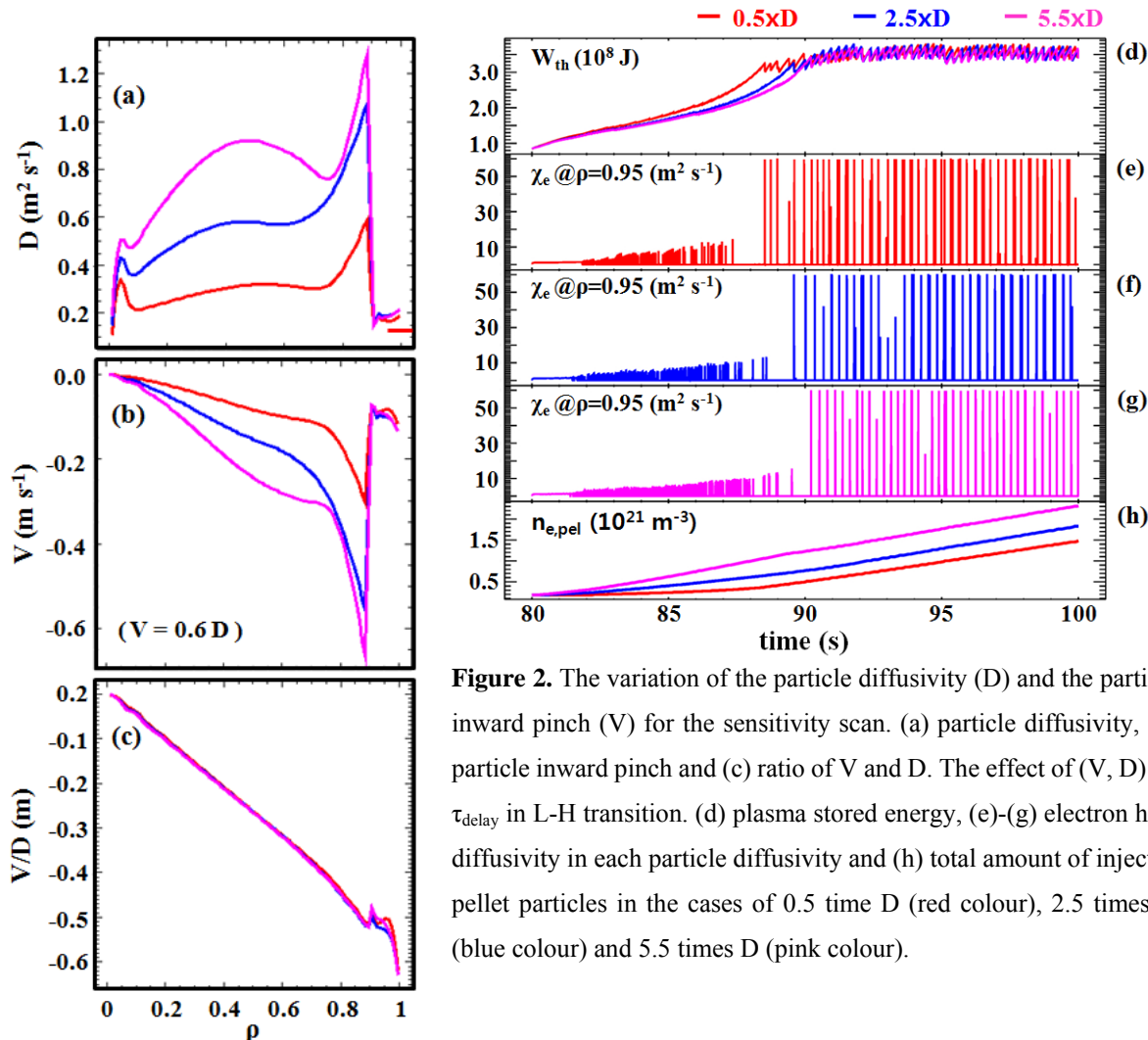


**Figure 2.** The variation of the particle diffusivity (D) and the particle inward pinch (V) for the sensitivity scan. (a) particle diffusivity, (b) particle inward pinch and (c) ratio of V and D. The effect of (V, D) on  $\tau_{delay}$  in L-H transition. (d) plasma stored energy, (e)-(g) electron heat diffusivity in each particle diffusivity and (h) total amount of injected pellet particles in the cases of 0.5 time D (red colour), 2.5 times D (blue colour) and 5.5 times D (pink colour).

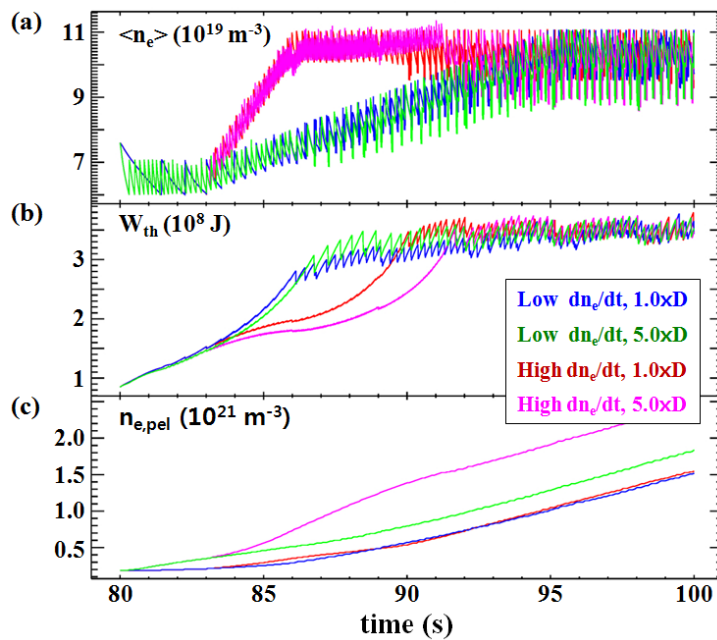


**Figure 3.** The combination effect of  $dn_e/dt$  and  $(V, D)$  on  $\tau_{\text{delay}}$  of L-H transition; (a) volume averaged electron density, (b) plasma stored energy, and (c) total amount of injected pellet particles in the cases of low  $dn_e/dt$  with low  $(V, D)$  (blue colour), low  $dn_e/dt$  with high  $(V, D)$  (green colour), high  $dn_e/dt$  with low  $(V, D)$  (red colour) and high  $dn_e/dt$  with  $(V, D)$  (pink colour).

Finally, the combined effect of both  $dn_e/dt$  and  $(V, D)$  to the characteristics of L-H transition is investigated. As shown in Fig. 3, the higher  $(V, D)$  profiles with the higher  $dn_e/dt$  presents the longest  $\tau_{\text{delay}}$ . In addition, the effect of  $(V, D)$  is maximized with the condition of high  $dn_e/dt$  in order to make the long  $\tau_{\text{delay}}$ .

**Summary.** In this work, the fully self-consistent predictive simulation of the typical ITER 15 MA scenario with  $Q = 10$  is performed for the flat top phase of the scenario. The characteristic time delay of reaching the burning conditions with  $Q = 10$  through L-H transition after onset of full heating is investigated with variation of  $dn_e/dt$  and  $(V, D)$ . This work shows that plasma fuelling by pellet injection is a powerful tool in controlling the speed of fusion power increase after L-H transition and the way of plasma evolution towards steady state burn in ITER.

## References

- [1] S. Wiesen et al, JET ITC-Report (2008)
- [2] Y. R. Martin et al, J. Phys.: Conf. Series 123, 012033 (2008)
- [3] L. Garzotti et al, Nucl. Fusion 52, 013002 (2012)
- [4] P. B. Snyder et al, Nucl. Fusion 51, 103016 (2011)